REVISION 1:

Crystal Structure and Hydration/Dehydration Behavior of a $Na_2Mg(SO_4)_2 \cdot 16H_2O$: a New Hydrate Phase Observed under Mars-Relevant Conditions

Kristin Leftwich[1], David L. Bish[1], C.H. Chen[2]

[1]Department of Geological Sciences, Indiana University, Bloomington, IN 47405, U.S.A.

[2]Indiana University Molecular Structure Center, Indiana University, Bloomington, IN 47405, U.S.A.

ABSTRACT

Hydrated evaporite minerals have the ability to hold large amounts of H_2O, making them a potential source of H_2O in cold, low-P_{H2O} environments such as the surface of Mars. Many of these hydrated evaporite minerals experience a reversible change in hydration state in response to changes in temperature (T) and relative humidity (RH). Such phases may thus have the potential to interact with the martian atmosphere on a daily or seasonal basis. The $Na_2Mg(SO_4)_2 \cdot nH_2O$ system was previously thought to contain three hydrated phases: a decahydrate (n = 10), konyaite (n = 5), and bl□dite (n = 4). We examined this system using temperature- and RH-controlled X-ray powder diffraction (XRD) methods, as well as temperature-controlled single-crystal X-ray diffraction. When bl□dite was exposed to sub-freezing conditions, T ≤ -10 °C, a new phase was produced (n = 16, 52 wt. %H_2O). Similar low-temperature behavior has been documented in the $MgSO_4 \cdot nH_2O$ system, through the presence of meridianiite (Peterson et al., 2007). The hydration and dehydration behavior of phases in the $Na_2Mg(SO_4)_2 \cdot nH_2O$ system was evaluated with powder XRD from -30 to >25 °C and from ~99 to near 0% RH, and single-crystal XRD data were collected for the n = 16 phase at -120 °C. The 16-hydrate is triclinic, space group P-1 {note to typesetting: P bar-over-one}, with unit-cell parameters a = 6.5590(12) Å, b = 6.6277(14) Å, c =

14.441(3) Å, α = 87.456(15)°, β = 79.682(15)°, γ = 65.847(13)° and a unit cell volume of 563.3(2) Å^3. The existence of this new phase at low temperatures, its high hydration state, and its ability to form reversibly from blödite all suggest that if phases in this system exist on the martian surface, they will participate in the Mars H_2O cycle.

Keywords: Mars, Sulfate, Bl□dite, Konyaite, Efflorescence, Meridianiite

INTRODUCTION

Limited liquid water stability on the martian surface suggests that hydration and dehydration of minerals with changes in temperature (T) and relative humidity (RH) during a Mars sol have the potential to influence the (bio)availability of water and potentially affect the atmospheric H_2O concentration. An increasing inventory of hydrous evaporite and silicate minerals has been identified from orbital and lander data on Mars (e.g., Ehlmann et al., 2009). Hydrous sulfate minerals are known to be present on Mars, based on spectral, chemical, and geomorphic observations (e.g., CRISM, OMEGA, and Mars Exploration Rover results). In the early 2000s, OMEGA/Mars Express imaged light patches in the martian soil, interpreted to be efflorescence. Spectral data indicated the presence of kieserite, gypsum, and polyhydrated sulfates, possibly epsomite, on the surface (Gendrin et al., 2005). Bassanite has also been suggested on Mars based on spectral data (Wray et al., 2010). Gypsum has been identified on the martian surface on many occasions using spectroscopic observations (e.g., Langevin et al., 2005; Squyres et al., 2012), and anhydrite was recently identified by the CheMin instrument in an aeolian bedform in Gale crater (Bish et al., LPSC, 2013). Sulfate minerals are of particular interest due to the ability of many of them to hydrate reversibly, some on the scale of a martian sol. For example, meridianiite ($MgSO_4 \cdot 11H_2O$) occurs only below 2 °C (Peterson et al., 2007) and incongruently melts above

that temperature to form less-hydrated $MgSO_4$ phases such as epsomite or hexahydrite (Chou and Seal, 2007).

Phases in the $Na_2MgSO_4 \cdot nH_2O$ system were predicted to occur on Mars by Clark and Van Hart (1981) based on X-ray fluorescence (XRF) chemical analyses on the Viking lander. King et al. (2004) also predicted phases in this system based on groundwater compositions of igneous rocks on Earth. Many of these groundwaters on Earth are concentrated in Mg, Ca, Na, K, SO_4, HCO_3/CO_3, and Cl. Evolution of these groundwaters, which should be acidic and sulfate-rich (Bishop et al. 2005), is predicted to form bl□dite based on the compositional diagram from King et al. (2004).

This study examined the behavior of solid phases in the Na-Mg-SO_4-H_2O system under Mars-relevant conditions to determine the potential for phases to participate in the martian H_2O cycle. Our experiments represent the first to describe this system's behavior under low-temperature conditions and are the first to describe this highly hydrated, low-temperature phase. Bl□dite was the starting material for all experiments, and no intermediate phases (between bl□dite and the newly described 16-hydrate phase) were observed during these experiments. Bl□dite ($Na_2MgSO_4 \cdot 4H_2O$) is the stable hydrate at room temperature, and it was analyzed by powder X-ray diffraction (XRD) under controlled RH-T conditions to investigate mineral reactions. When bl□dite was exposed to low temperatures ($T < 0$ °C), two different results were observed. One set of experiments produced a higher hydrate in the $Na_2MgSO_4 \cdot nH_2O$ system, which was investigated via powder and single-crystal XRD methods. The resulting data were used to define experimental stability conditions and the crystal structure of the new phase. Other experiments resulted in reaction of bl□dite to form two single-cation salts.

EXPERIMENTAL METHODS

69 **Powder X-ray Diffraction**

70 A natural bl□dite sample from Soda Lake, California, was used for all analyses. XRD data
71 were obtained for dry samples and for those that had been previously deliquesced in a 100% RH
72 chamber (all natural bl□dite samples showed no evidence of having deliquesced prior to our
73 experiments and were pure blödite). Powder XRD data were obtained at Indiana University in the
74 Department of Geological Sciences using a Bruker D8Advance diffractometer with a Vantec
75 position-sensitive detector (Cu radiation: $\lambda = 1.5406$ Å). Data were collected using a variety of 2θ
76 ranges, mostly between 15-55°, all with a step size of 0.01682°, a variety of scan speeds (0.45 -
77 1.0 sec/step), and a 0.6 mm divergence slit. This instrument is equipped with an Anton-Paar TTK
78 450 temperature-control stage that was used for measurements under non-ambient, RH- and T-
79 controlled conditions to produce the experimental stability diagrams. Cooling was achieved by
80 circulation of chilled methanol through the base of the stage, and sample temperature was held
81 constant using the heater of the TTK stage. The sample stage is contained within an
82 environmental cell that can be open to air, put under vacuum, or exposed to controlled RH.
83 Controlled-RH conditions were generated using an InstruQuest V-Gen dew point/RH generator.
84 Roughing-pump vacuum conditions were also used for generating low-RH conditions for low-
85 temperature (-30 to -50 °C) experiments. The RH for these experiments was calculated using the
86 room P_{H2O} (determined by measuring room RH and T) at 1 atm using Equation 1. The V-Gen RH
87 generator is designed to produce RH values as low as 1% RH, although we successfully operated
88 to ~0.5% RH. Controlled-RH conditions ≤ 0.5% at room temperature were required for
89 experiments below -30 °C, and we used a roughing pump to lower the environmental chamber
90 pressure on both dry and humid days for these measurements.

91 $$P_{H2O,vac} = P_{H2O,rm}\left(\frac{P_{vac}}{P_{room}}\right) \quad \text{(Equation 1)}$$

The rates of hydration/dehydration reactions are important in determining whether the reactions have the potential to contribute to the martian diurnal H_2O cycle. Thermogravimetric analysis (TGA) is often used to study the dehydration reaction kinetics of minerals, but we did not have access to an instrument that allowed control of both RH and T at sub-ambient temperatures. As an alternative, we used time-resolved XRD in an attempt to quantify the rates of hydration and dehydration reactions. These measurements used the Vantec detector in fixed-detector mode (6° 2θ detector window), making an individual measurement every 20 sec while monitoring RH and T. RH was set to a fixed value (at 23 ± 0.5 °C) while slowly decreasing T from 0 °C to -40 °C (thereby causing an increase in RH over the specimen) in order to study hydration rates. These data were intended to provide information on abundances of phases (through Rietveld analysis) as a function of temperature. Unfortunately, formation of the new phase in the mount caused significant preferred orientation, adversely affecting quantitative analyses and making these measurements unsuitable for kinetic studies.

Single-Crystal X-ray Diffraction

Data used in the determination of the structure of the 16-hydrate phase were obtained using a Bruker Kappa ApexII Duo diffractometer (Mo radiation: λ = 0.7107 Å) at the Indiana University Molecular Structure Center (IUMSC). Data were collected while the crystal was under a nitrogen cold stream at -123 °C. The sample used was previously deliquesced, natural bl□dite from Soda Lake, CA. This deliquesced sample was stored in a freezer at -10 °C (RH buffered by ice to 100%RH) for two weeks prior to analysis. The approximately 0.5 x 0.2 x 0.1 mm crystal was mounted at room temperature, having been exposed to room RH and T (average 23-24 °C, 30-40% RH) for less than 10 min before being mounted onto a MiTeGen micromount under a cold nitrogen stream. The RH during the single-crystal experiment is unknown, but the cold stream

was not contained within an environmental cell, allowing it to mix with the surrounding air. Thus the RH was apparently high enough to keep the crystal hydrated; at the temperature of the sample, very little H_2O is required to reach high effective relative humidities.

Chemical Analysis

Powder XRD data for the starting bl□dite sample showed no evidence of any additional phases, although the sample is dark colored. The chemical composition of the bl□dite sample used for all experiments was measured by atomic absorption spectroscopy using a Perkin Elmer AAnalyst 800 for cation concentrations and an Eltra CS-200 elemental analyzer for total carbon (TC) and total sulfur (TS). An aliquot of the original sample was dissolved with nitric acid and diluted for graphite furnace analysis (AAnalyst). This solution was used to analyze for K, Ca, and Fe, and all were present at $<6 \times 10^{-3}$ mol element per mol bl□dite. An Eltra CS-2000 elemental analyzer was used for total carbon (TC) concentration determination, yielding a TC concentration of 0.054 wt. % (σ=0.0001 wt. %). Our interpretation of the TC measurements is that the source of the color was admixed organic material, although the source is unimportant at this low concentration. These data support the assumption that any non-bl□dite material did not contribute to the overall chemistry of the sample.

RESULTS

$Na_2Mg(SO_4)_2 \cdot 16H_2O$

New diffraction peaks were observed when bl□dite was exposed to -10 °C and analyzed via time-resolved X-ray powder diffraction (47-78% RH). These new peaks persisted at temperatures as low as -123 °C (as evidenced by the single-crystal diffraction measurements). In an attempt to explain these peaks, the structures of potential reaction products listed in Table 1 were used to perform Rietveld analysis of the powder data in Bruker's TOPAS program. The poor fit of these known phases to the data led us to conclude that the unexplained peaks represented a new phase.

Structure determination by powder diffraction was attempted, but the rates of the hydration reaction were such that it was difficult to obtain a sample with only the 16-hydrate crystalline phase. In addition, the XRD intensities were affected by preferred orientation created when the phase crystallized in situ. Single-crystal methods were therefore employed for solution of the structure. Crystals of the 16-hydrate were formed by first allowing bl□dite to deliquesce in a 100%RH atmosphere at room temperature. This material was then stored in a -10 °C freezer, resulting in crystallization of the 16-hydrate. Once mounted, the single crystal was allowed to cool to -123 °C in an N_2 stream for approximately thirty min prior to data collection while several indexing attempts were made. Indexing gave a symmetry and unit cell inconsistent with bl□dite. The crystal remained in the N_2 stream for an additional thirty min to allow the sample to equilibrate before data collection began. Initial indexing of the single-crystal data gave space group P-1 {note to typesetting: same as in intro} with unit-cell parameters of a ≅ 6.56 Å, b ≅ 6.63 Å, c ≅ 14.4 Å, α ≅ 87.4°, β ≅ 79.7°, γ ≅ 65.9°, yielding a unit cell volume ≅ 563 $Å^3$. These preliminary results were used with the original powder XRD data to perform a Le Bail refinement, shown in Figure 1.

The single-crystal data were analyzed using the charge-flipping method with Oxford Crystals (Betteridge et al, 2003) for structure solution. Table 2 shows the unit-cell parameters of the triclinic (P-1) structure and atom positions from the single-crystal structure solution. This structure was determined using 2,537 reflections (GooF = 0.9339, R_w = 10.97% and R = 3.91%). A stoichiometry of $Na_2Mg(SO_4)_2$ was used for this solution and all Na and Mg cations and sulfate tetrahedra were identified. H_2O molecules were assigned to unidentified electron density on difference-Fourier maps, similar to the process used by Peterson and Wang (2006) for the meridianiite crystal structure solution. O-H bond lengths for the 16-hydrate were constrained

based on the neutron diffraction structure of meridianiite at a comparable temperature (Fortes, 2008). Table 3 shows a calculated XRD pattern for this material.

Structure solution yielded a formula of $Na_2Mg(SO_4)_2 \cdot 16H_2O$; as noted above, this hydration state was not confirmed by TGA. Figure 2 compares the crystal structures of blödite and the 16-hydrate. Mg and Na are octahedrally coordinated by H_2O molecules, creating planes of octahedra. The 16-hydrate structure contains independent sulfate tetrahedra with alternating up/down orientations along the *b* axis between these planes of octahedra. Isolated H_2O molecules are H-bonded to the sulfate oxygen atoms.

Bond distances were compared with those from published crystal structures having similar bonding environments to evaluate the 16-hydrate structure (Table 4). Published bond distances for meridianiite and mirabilite were used to evaluate S-O distances for the 16-hydrate. The average S-O distance in meridianiite is 1.451 Å (Fortes et al., 2008), 1.463 Å in mirabilite (Levy and Lisensky, 1978), and 1.477 Å in the 16-hydrate. Mg-O distances and Na-O distances in the 16-hydrate were compared with those in bl□dite (Hawthorne, 1985). The average Mg-O distance in bl□dite is 2.076 Å vs. 2.057 Å for the 16-hydrate. Na-O bonds yielded similar results, with 2.421 Å in bl□dite and 2.418 Å in the 16-hydrate. The temperature of data collection for blödite was not reported and was assumed to have been 22 °C. The low-temperature collection of the 16-hydrate data may account for small observed differences in bond lengths.

The single-crystal structure was subsequently used in a Rietveld refinement with the powder XRD data, yielding a unit cell similar to that of the initial TOPAS Le Bail refinement. The 16-hydrate phase crystallized in the mount during the experiment, producing a sample with a high degree of preferred orientation. Therefore a fourth-order spherical-harmonics preferred orientation correction was used in the refinements. Results of the Rietveld refinement are shown in Figure 3.

The experimental setup described previously (i.e., TTK stage and V-Gen) was used to expose this mineral to a range of conditions in RH/T space, and XRD data were measured for these conditions. Only bl□dite was present under conditions represented by gray dots, and black boxes indicate the presence of the 16-hydrate phase. The shaded area in Figure 4 represents the range of RH/T conditions measured by the Viking lander 1 (Savijärvi, 1995). Konyaite and the decahydrate phase were not observed in any measurement.

In an attempt to produce only the 16-hydrate, experiments were performed by storing bl□dite (either dry or in deliquesced mush form) at -10 °C for several days in a freezer. These experiments sometimes produced a mixture of mirabilite ($Na_2SO_4 \cdot 10H_2O$; 56 wt. % H_2O) and a hydrous $MgSO_4$ phase, either meridianiite ($MgSO_4 \cdot 11H_2O$; 62 wt. % H_2O) or epsomite ($MgSO_4 \cdot 7H_2O$; 51 wt. % H_2O), depending on RH and T conditions. Circumstantial evidence (e.g., high background and insufficient $Na_2(SO_4)$ phases to account for initial stoichiometry, determined through Rietveld analysis) for amorphous sodium sulfate in association with epsomite was also observed under lower-RH conditions.

DISCUSSION

RH and T are critical independent variables determining hydrous mineral stability, especially in low-P_{H2O} conditions. However, although observation of new phases may indicate relative thermodynamic stability of phases, the rates of reactions at the low temperatures found on the martian surface may be sufficiently slow that the reaction times used here were insufficient to yield the true stable phase assemblage. For this reason, we refer to Figure 4 as an experimental stability diagram. The RH-T cycle over a Mars late summer day ~23 °N of the equator is represented by the shaded area on Figure 4, as observed by the Mars Viking lander 1 (Savijärvi, 1995). This region is encompassed by the projected experimental stability field of the 16-hydrate

208 phase, suggesting that this phase would be stable under conditions occurring in the martian mid-
209 latitude regions. The highest reported temperature from the Phoenix lander, at ~ 68 °N, is ~ -23
210 °C, with temperatures down to ~ -82 °C (Zent et al., 2010). Our data suggest that the
211 hydration/dehydration reaction would not occur at these higher latitudes and instead the hydrated
212 phase would be the stable phase in this system. The Curiosity REMS (Rover Environmental
213 Monitoring Station) instrument, which landed ~ 5 °S of the equator, has returned temperature data
214 as high as 8 °C (marsweather.com/data). Bl□dite is the stable phase at this temperature, but the
215 REMS instrument has also recorded temperatures as low as -78 °C. This temperature is well
216 within the stability field of the 16-hydrate, suggesting that phases in this system could transform
217 on a diurnal cycle if they exist in Gale Crater. Indeed, even small amounts of such phases (<<1%)
218 could potentially responsible for the weak cementation that has been observed in some martian
219 surficial deposits.

220 Whether the 16-hydrate phase is truly thermodynamically stable is questionable; approximately
221 20 - 30% of the experiments in which RH/T conditions favored the 16-hydrate phase resulted
222 instead in formation of two single-cation salts. The separation of the system into two phases could
223 be interpreted to indicate that the single-cation salts are thermodynamically preferred at these low
224 temperatures. Alternatively, Spencer (2000) suggested that bl□dite is more soluble than epsomite
225 and thenardite at room temperature. This implies the separation could have occurred between
226 analyses, during storage at room temperature as a deliquesced solution. Each aliquot of sample
227 was reused for several low-temperature XRD analyses, and in some cases, aliquots were only
228 analyzed and confirmed to be bl□dite when the sample was first put into the XRD sample mount.
229 These were not reanalyzed at room temperature between individual low-temperature experiments.
230 It is possible that the presence of two single-cation phases reflects instability of bl□dite during

storage at room temperature, rather than the lack of stability of the 16-hydrate at the RH/T conditions of interest as mineralogy was not monitored prior to or during the cooling process. As the system contained the 16-hydrate throughout prolonged low-temperature experiments, we believe that it is likely a stable phase and that in some cases bl□dite had converted to two phases before the experimental trial commenced.

Konyaite and decahydrate did not participate in the hydration/dehydration cycles in our experiments. The decahydrate (Leduc et al., 2009) forms when this system first produces a crystalline phase from solution under average Earth-surface conditions. This phase readily dehydrates to konyaite and then to the stable phase at these conditions, bl□dite. Hydration of bl□dite at room temperature was not observed, despite exposure to RH values approaching saturation. However, when exposed to high RH values at low temperature, hydration of bl□dite in our experiments bypassed these intermediate hydrates and formed the 16-hydrate. Dehydration of this phase to bl□dite when exposed to temperatures above -10 °C yields a ~ 39 wt. % loss due to release of H_2O. This large H_2O loss illustrates the capacity of this system to store significant H_2O, making these phases another potential source of episodic liquid water on the surface of Mars.

The rates of these reactions are sufficiently rapid that this hydration/dehydration cycle would occur at the equator on the time scale of a martian sol, based on the observed hydration of samples stored at low temperatures (-21 °C) overnight (<12 hrs). The dehydration reaction would be expected to occur wherever the daytime T exceeded -10 °C. If phases in the $Na_2Mg(SO_4)_2$-H_2O system occur on Mars, as suggested by Clark and Van Hart (1981) and King et al. (1984), our results show that hydration/dehydration reactions between the 4- and 16-hydrate will occur over much of the martian surface and that the 16-hydrate would be the stable phase in polar regions.

ACKNOWLEDGEMENTS

This research was supported by a NASA Mars Fundamental Research grant to DLB supporting the study of hydrous minerals on Mars. Thanks also go to M. Pink, L. Wasylenki, E. Elswick, and R. Wintsch for their guidance and contribution to this paper.

REFERENCES

Bishop, J.L., Dyar, M.D., Lane, M.D., and Banfield, J.F. (2005) Spectral identification of hydrated sulfates on Mars and comparison with acidic environments on Earth. International Journal of Astrobiology, 3.4, 275-285.

Betteridge, P.W., Carruthers, J.R., Cooper, R.I., Prout, K., and Watkin, D.J. (2003) Oxford Crystals. Journal of Applied Crystallography, 36, 1487.

Bish, D.L., Blake, D.F., Vaniman, D.T., Chipera, S.J., Sarrazin, P., Morris, R.V., Ming, D.W., Treiman, A.H., Downs, R.T., Achilles, C., Morrison, S., Yen, A., Brisow, T., Morookian, J., Farmer, J., Crisp, J., Rampe, E., Stolper, E., Des Marais, D., Spanovich, N., Anderson, R., and the MSL Science Team. First X-ray diffraction results from Mars Science Laboratory: Mineralogy of Rocknest aeolian bedform at Gale crater. (2013) 44th Lunar and Planetary Science Conference, Abstract #1111

Bruker (2007) *TOPAS, EVA*. Bruker AXS Inc., Madison, Wisconsin, USA.

Brandenburg, K. Diamond version 3.2i. Crystal Impact GbR. Bonn, Germany. June 2012.

Chou, I.M. and Seal R.R. (2007) Magnesium and calcium sulfate stabilities and the water budget of Mars. Journal of Geophysical Research, Planets, 112, E11.

Clark, B.C. and Van Hart, D.C. (1981) The salts of Mars. Icarus, 45, 370-378.

Ehlmann, B.L., Mustard, J.F., Swayze, G.A., Clark, R.N., Bishop, J.L., Poulet, F., Des Marais, D.J., Roach, L.H., Milliken, R.E., Wray, J.J., Barnouin-Jha, O., and Murchie, S.L. (2009) Identification of hydrated silicate minerals on Mars using MRO-CRISM: Geologic context near Nili Fossae and implications for aqueous alternations. Journal of Geophysical Research, 114, E00D08.

Fortes, A.D., Wood, I.G., and Knight, K.S. (2008) The crystal structure and thermal expansion tensor of $MgSO_4 \cdot 11D_2O$ (meridianiite) determined by neutron powder diffraction. Physics and Chemistry of Minerals, 35, 207-221.

Gendrin, A., Mangold, N., Bibring, J., Langevin, Y., Gondet, B., Poulet, F., Bonello, G., Quantin, C., Mustard, J., Arvidson, R., and LeMouélic, S. (2005) Sulfates in martian layered terrains: The OMEGA/Mars Express view. Science, 307, 1587-1591.

Hawthorne, F.C. (1985) Refinement of the crystal structure of bloedite: Structural similarities in the [M(T_4)2_n] finite-cluster minerals. Canadian Mineralogist, 23, 669-674.

King, P.L., Lescinsky, D.T., and Nesbitt, H.W. (2004) The composition and evolution of primordial solutions on Mars, with application to other planetary bodies. Geochimica et Cosmochimica Acta, 68.23, 4993-5008.

Langevin, Y., Poulet, F., Bibring, J.P., and Gondet, B. (2005) Sulfates in the north polar region of Mars detected by OMEGA/Mars Express. Science, 307, 1584-1586.

Leduc, E.M.S., Peterson, R.C., and Wang, R. (2009) Sodium magnesium sulfate decahydrate, $Na_2Mg(SO_4)_2 \cdot 10H_2O$, a new sulfate salt. Acta Crystallographica, C65, i81-i84.

Levy, H.A., and Lisensky, G.C. (1978) Crystal structures of sodium sulfate decahydrate (Glauber's salt) and sodium tetraborate decahydrate (borax). Redetermination by neutron diffraction. Acta Crystallographica, B34, 3502-3510.

Peterson, R.C., Nelson, W., Madu, B., and Shurvell, H.F. (2007) Meridianiite: A new mineral species observed on Earth and predicted to exist on Mars. American Mineralogist, 92, 1756-1759.

Peterson, R. C. and Wang, R. (2006) Crystal molds on Mars: Melting of a possible new mineral species to create Martian chaotic terrain. Geology, 34, 957-960

Savijärvi, H. (1995) Mars boundary layer modeling: Diurnal moisture and soil properties at the Viking Lander 1 site. Icarus, 117, 120-127.

Spencer, R.J. (2000) Sulfate minerals in evaporite deposits. Reviews in Mineralogy and Geochemistry, 40, 173-192.

Squyres, S.W., Arvidson, R.E., Bell, J.F., Calef, F., Clark, B.C., Cohen, B.A., Crumpler, L.A., de Souza, P.A., Farrand, W.H., Gellert, R., Grant, J. Herkenhoff, K.E., Hurowitz, J.A., Johnson, J.R., Joliff, B.L., Knoll, A.H., Li, R., McLennan, S.M., Ming, D.W., Mittlefehldt, D.W., Parker, T.J., Paulsen, G., Rice, M.S., Ruff, S.W., Schroder, C., Yen, A.S., and Zacny, K. (2012) Ancient impact and aqueous processes at Endeavour Crater, Mars. Science, 336, 570-576.

Wray, J.J., Squyres, S.W., Roach, L.H., Bishop, J.L., Mustard, J.F., and Dobrea, E.Z.N. (2010) Identification of the Ca-sulfate bassanite in Mawrth Vallis, Mars. Icarus, 209, 416-421.

Zent A.P. Hecht, M.H., Cobos, D.R., Wood, S.E., Hudson, T.L, Milkovich, S.M., DeFlores, L.P., and Mellon, M.T. (2010) Initial results from the thermal and electrical conductivity probe (TECP) on Phoenix. Journal of Geophysical Research Planets, 115, EOOE14.

REVISION 1:

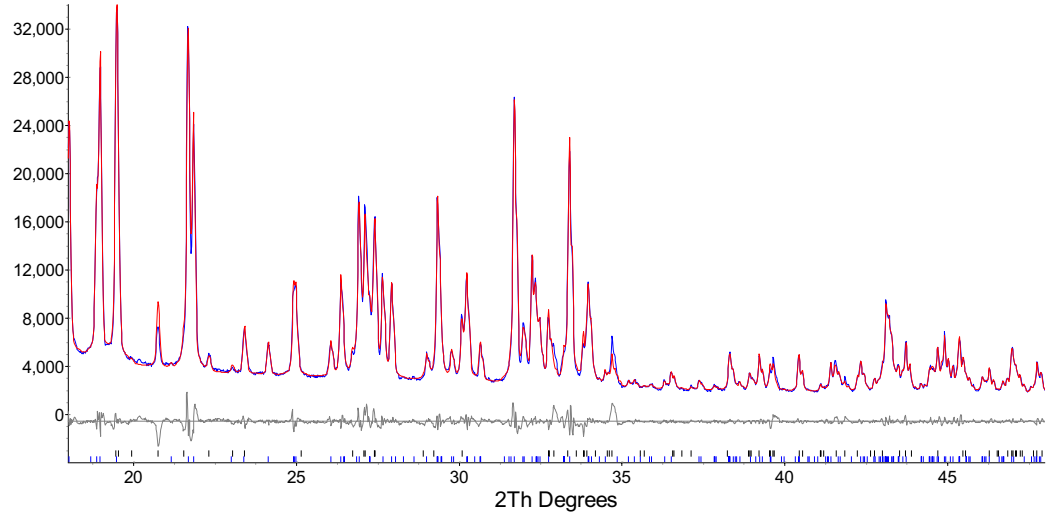

Figure 1: Results of Le Bail refinement using space group P-1 determined from single-crystal methods to fit previously unexplained peaks (blue: observed data; red: Le Bail fit; grey (below): difference). Vertical tic marks at the bottom of the plot represent the theoretical positions of blödite (black) and 16-hydrate reflections (blue).

Table 1: Crystalline phases used in Rietveld analysis			
Phase Name	Formula	**Phase Name**	Formula
Blödite	$Na_2Mg(SO_4)_2{\cdot}4H_2O$	**Hexahydrite**	$MgSO_4{\cdot}6H_2O$
Konyaite	$Na_2Mg(SO_4)_2{\cdot}5H_2O$	**Epsomite**	$MgSO_4{\cdot}7H_2O$
Decahydrate	$Na_2Mg(SO_4)_2{\cdot}10H_2O$	**Meridianiite**	$MgSO_4{\cdot}11H_2O$
Kieserite	$MgSO_4{\cdot}H_2O$	**Löweite**	$Na_{12}Mg_7(SO_4)_{13}{\cdot}15H_2O$
Sanderite	$MgSO_4{\cdot}2H_2O$	**Matteuccite**	$NaHSO_4{\cdot}H_2O$
Starkeyite	$MgSO_4{\cdot}4H_2O$	**Vanthoffite**	$Na_6Mg(SO_4)_4$
Pentahydrate	$MgSO_4{\cdot}5H_2O$	**Thenardite**	Na_2SO_4
Ice	H_2O	**Mirabilite**	$Na_2SO_4{\cdot}10H_2O$

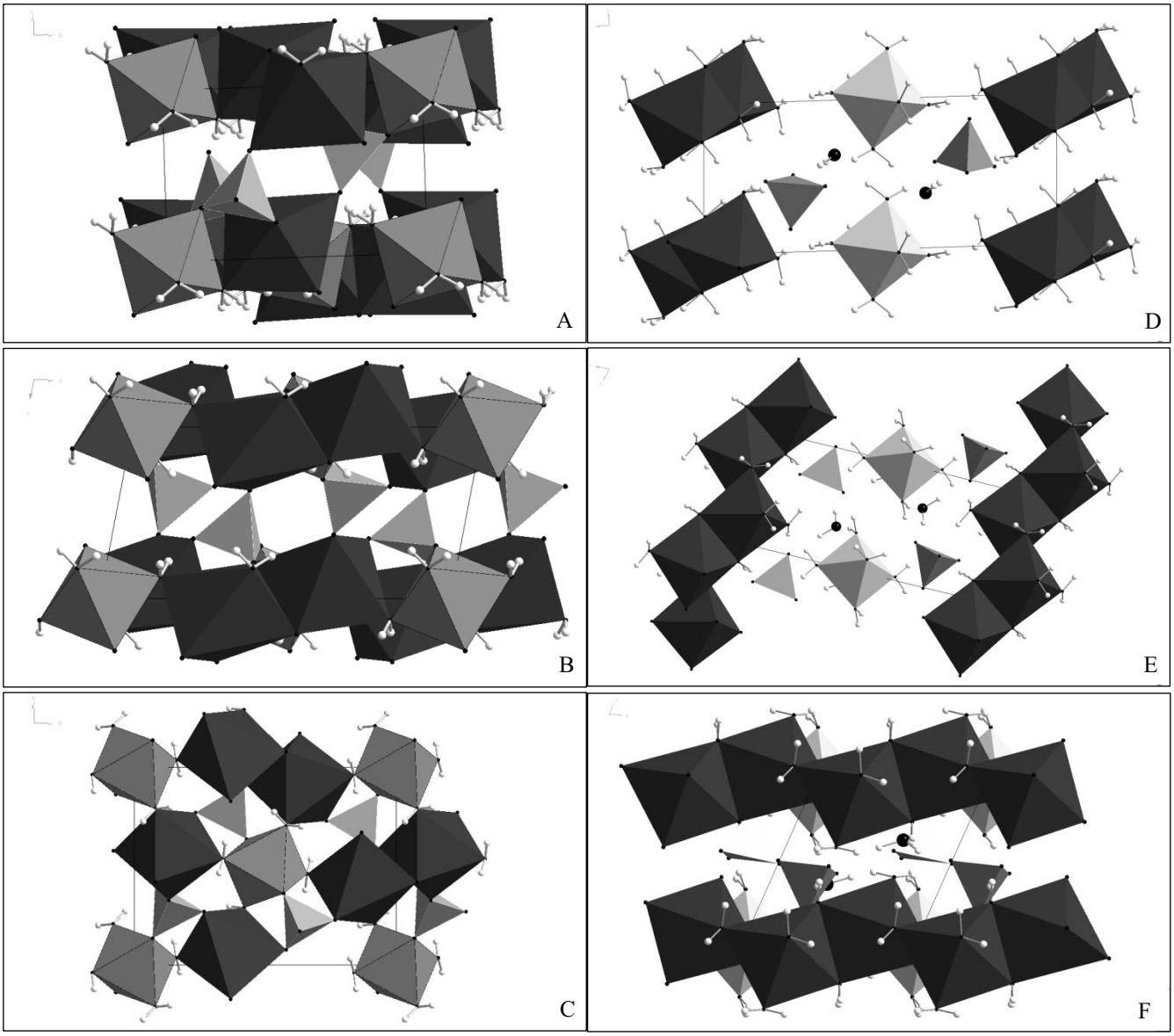

Figure 2: Comparison of blödite (left) and 16-hydrate (right) structures. Left images are projections down the *a* (A), *b* (B), and *c* (C) axes of blödite. Darker octahedra represent Na atoms octahedrally coordinated by H_2O. Lighter grey octahedra represent Mg atoms octahedrally coordinated by H_2O. Grey tetrahedra are sulfate (SO_4) tetrahedra coordinated by O. Right images are projections down the *a* (D), *b* (E), and *c* (F) axes of the 16-hydrate. As in the blödite images, Na octahedra are in a darker grey than Mg octahedra, and sulfate tetrahedra are in a medium hue. Note isolated H_2O molecules between cation layers.

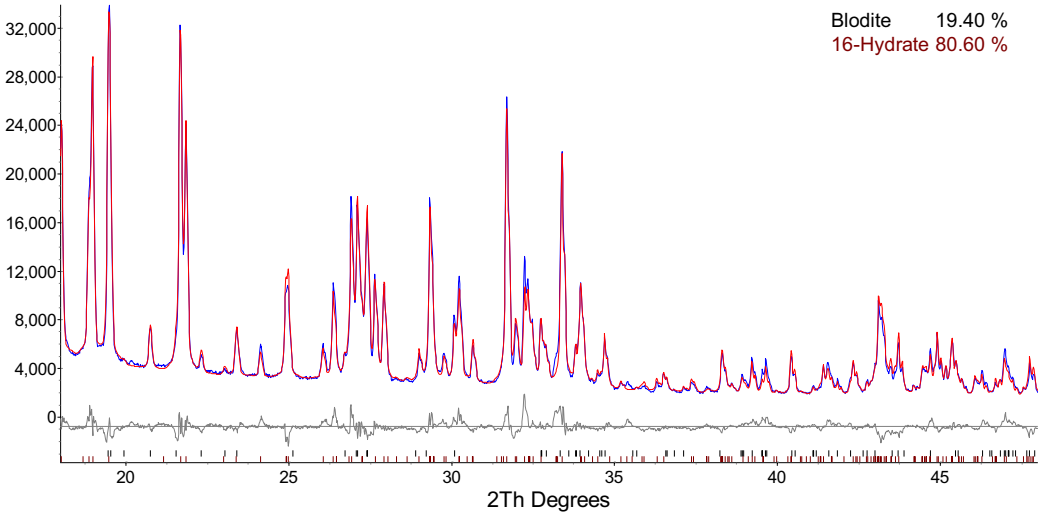

Figure 3: Rietveld analysis of powder XRD data using the single-crystal structure data; blue: observed data; red: model pattern; black: difference. Vertical tic marks at the bottom of the plot represent the theoretical positions of blödite (black) and 16-hydrate (brown) reflections.

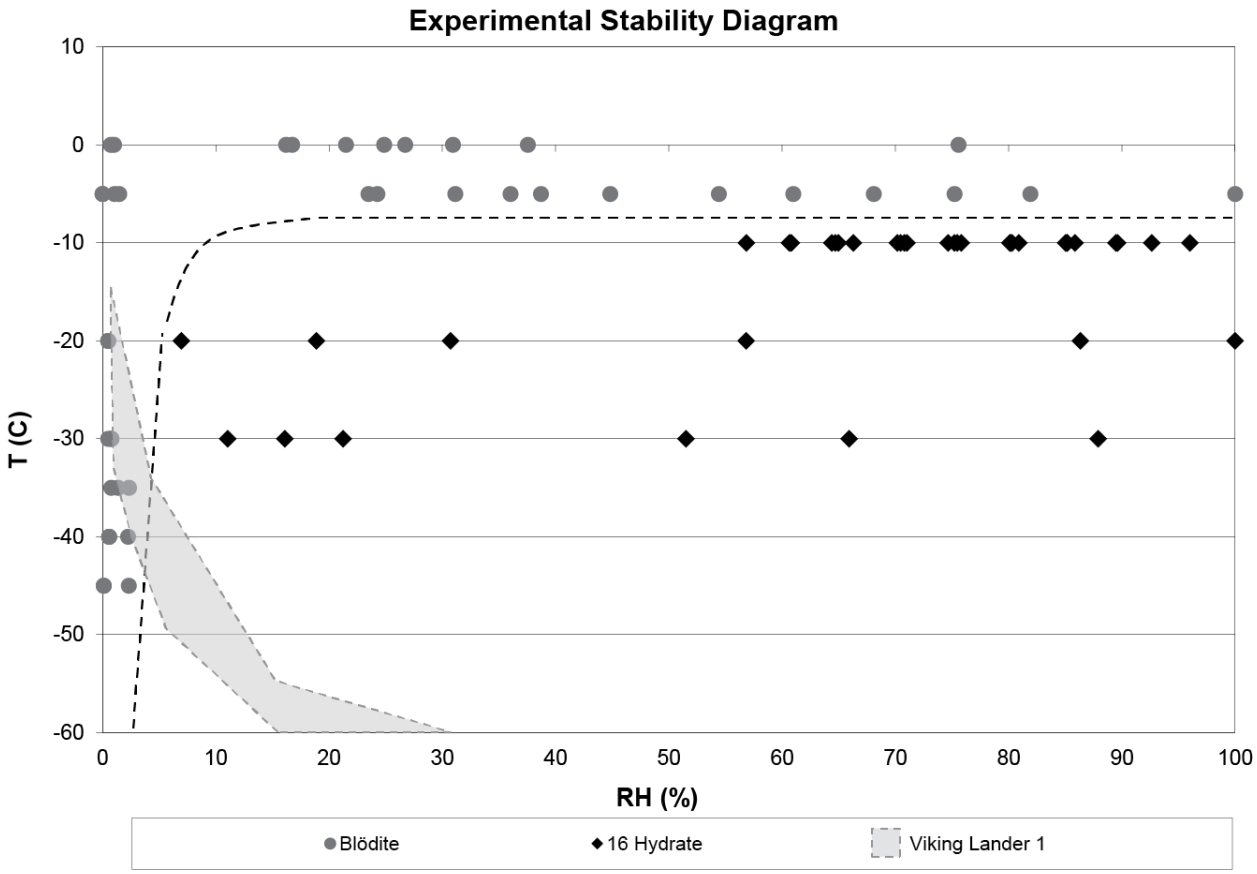

Figure 4: RH/T data showing occurrences of blödite and the 16-hydrate phase, with Viking lander 1(Savijärvi, 1995) RH/T data overlain.

Table 2: Unit-Cell Parameters, Isotropic Displacement Parameters, and Atom Positions for $Na_2Mg(SO_4)_2 \cdot 16H_2O$

***a* (Å)**	6.559(1)	***α* (°)**	87.46(2)
***b* (Å)**	6.628(1)	***β* (°)**	79.68(2)
***c* (Å)**	14.441(3)	***γ* (°)**	65.85(1)

Atom	x	y	z	U_{iso}
Na	0.2484(2)	0.9483(2)	0.04994(7)	0.017
Mg	0	0	0.5	0.014
S	0.7611(1)	0.6075(1)	0.25526(4)	0.012
O1	0.7023(3)	0.8471(3)	0.2467(1)	0.017
O2	0.6359(3)	0.5698(3)	0.3449(1)	0.018
O3	0.0080(3)	0.4899(3)	0.2537(1)	0.017
O4	0.6996(3)	0.5250(3)	0.1757(1)	0.019
O5	0.3213(3)	0.9745(3)	0.4464(1)	0.019
O6	-0.0307(3)	0.9505(3)	0.3623(1)	0.021
O7	0.1216(3)	0.6675(3)	0.5202(1)	0.019
O8	0.2930(3)	0.5923(3)	0.1141(1)	0.019
O9	0.3324(3)	0.2516(3)	-0.0048(1)	0.021
O10	0.1614(3)	0.9057(3)	-0.1004(1)	0.019
O11	0.2517(3)	0.0390(3)	0.2102(1)	0.019
O12	0.3352(3)	0.3641(3)	0.3709(1)	0.022
H1	0.288(7)	0.351(5)	-0.057(2)	0.05*
H2	0.398(4)	0.994(6)	0.230(3)	0.05
H3	0.202(6)	0.603(6)	0.572(2)	0.05
H4	0.204(7)	0.989(6)	-0.151(2)	0.05
H5	0.446(5)	0.844(4)	0.415(2)	0.05
H6	0.425(4)	0.562(6)	0.142(2)	0.05
H7	0.286(7)	0.377(4)	0.039(2)	0.05
H8	-0.154(5)	0.948(7)	0.335(3)	0.05
H9	0.457(5)	0.409(6)	0.347(3)	0.05
H10	0.224(5)	0.428(6)	0.331(2)	0.05
H11	0.347(7)	0.100(4)	0.419(3)	0.05
H12	0.070(5)	0.966(6)	0.308(2)	0.05
H13	0.188(5)	0.581(7)	0.167(2)	0.05
H14	0.202(6)	0.564(5)	0.467(2)	0.05
H15	0.175(6)	0.198(3)	0.224(3)	0.05
H16	0.198(7)	0.767(4)	-0.131(2)	0.05

*All H-atom displacement parameters were fixed at 0.05.

Table 3: Calculated XRD pattern for the 16-hydrate

Intensity (arbitrary)	*d* (Å)	*h*	*k*	*l*
333	5.498	0	1	1
631	5.367	1	1	1
674	5.13	-1	0	1
348	4.898	-1	-1	1
530	4.677	0	-1	2
492	4.655	1	1	2
826	4.53	0	1	2
624	4.081	-1	-1	2
1000	4.06	1	0	3
348	3.555	-1	1	0
363	3.289	1	2	0
273	3.183	1	1	4
431	3.031	1	-1	3
689	3.02	0	2	0
639	2.945	2	0	0
687	2.812	-1	-1	4
293	2.749	0	2	2
695	2.67	1	1	5
380	2.085	-1	-3	2
275	2.064	-3	-1	1